Multi-scale investigation of dislocation mediated carbon migration in iron

Tigany Zarrouk

August 6, 2020

Contents

1 Introduction **2**

2 Computational Method **4**

3 Results **4**
3.1 Peierls Potential 4
3.2 Hard and easy core relaxations 8
3.3 Line Tension 13

4 Discussion **15**

5 Future work **16**

6 Conclusion **16**

7 Appendix **17**
7.1 Regularisation of interaction energy in quadrupolar array . . 17

8 Bibliography **17**

Abstract

We investigate the validity of a dislocation-assisted carbon migration mechanism underpinning the formation of dark etching regions in bearing steels undergoing high-cycle fatigue through use of a multi-scale approach: from quantum mechanics, to stochastic simulations. We start from tight binding simulations of $1/3\langle 111\rangle$ screw dislocations to obtain the 2-d Peierls potential and Fe-C binding energies. These become ingredients for a line-tension model of the $1/3\langle 111\rangle$ screw dislocation to obtain the kink-pair formation energy as a function of stress and carbon concentration. Finally, 3-d kinetic Monte-Carlo simulations of dislocations in an environment of carbon are used to ascertain which temperature and stress regimes dislocation-assisted carbon migration is a valid mechanism.

1 Introduction

Martensitic steels are frequently used in bearings due to their resilience to service conditions, being subject to high rotational speeds and contact pressures. However, under cyclic loading exceeding a given contact stress, the microstructure of the steel can decay due to the accumulation of plasticity. This signals the onset of rolling cycle fatigue (RCF), which increases the risk of failure from subsurface crack initiation. The microstructural decay corresponds to the observation of Dark Etching Regions (DERs) as seen in optical microscopy, where the darkness of these regions is due to the higher reactivity of the phases which compose the DER to the etchant; exacerbated by the roughness of the DER region.

Carbon within the martensitic matrix at normal operating temperatures has a low diffusivity; as such it cannot segregate out of the martensite. A plausible mechanism for the degradation of the martensitic microstructure is a process of carbon migration, driven by dislocation glide, described as follows [CITATION]. Due to the high dislocation density exhibited in martensite, carbon segregates to dislocations in Cottrell atmospheres, causing pinning. Strain generated by cyclic stresses allow dislocations to escape their carbon rich environment. The dislocations, now free, re-attract carbon, allowing the Cottrell atmosphere to reform, subsequently re-pinning the dislocations, creating a net carbon flux.

structure of a WEB consisting of a ferrite band and a LC adjacent to it. One can see the DER region is composed of regions of ferrite interspersed in the parent martensite with lenticular carbides bordering the ferrite bands.

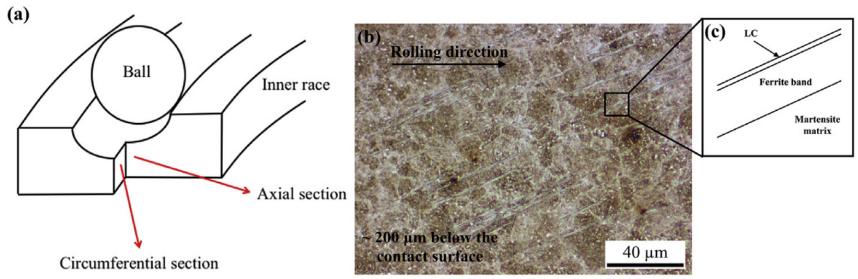

Figure 1: Diagram of where DER occurs and its characteristics, taken from [1]. (a) Axial and Circumferential sections of a bearing inner ring. (b) Circumferential section of a bearing inner ring under optical microscope, where ferrite bands (white etching bands) are formed at the subsurface with an inclination angle of 30° to the rolling direction. (c) Diagram showing the

Through dislocation-assisted carbon migration, martensite transforms to ferrite (microband and elongated forms). Residual carbides, untouched at the start of DER formation, gradually dissolve as a result of highly localised

plasticity: dislocation rearrangement and pile ups at the interface draw carbon atoms out. Further RCF progression leads to the formation of low and high angle ferrite features, White Etching Bands (WEBs), composed from the microband and elongated ferrite. Carbon migration through dislocation motion allows carbon to move from the martensitic matrix—and (partially) dissolved residual carbides—to form lenticular carbides between these ferrite bands.

However, fundamentals behind DER formation through this process remain contentious. It is not definitively known where carbon migrates to with the onset of DER formation: where does excess carbon from the martensitic matrix find itself, when the structure decays to low solubility (0.02%) ferrite? It is not known whether carbon atoms inside the martensite are transported towards the residual transition carbides, [2], or if they segregate to the boundaries of ferrite microbands/elongated ferrite.

Fu *et al.* propose that carbon atoms inside the martensite would segregate to pre-existing/residual carbides, increasing their size [2]. This theory has been successfully applied to the growth of lenticular carbides [1], however, problems arise with their application to the growth of residual carbides: if carbides were to form in martensite, they should follow the Bagaryatskii/Isaichev orientation relationship, but observations suggest a lack of any orientation relationship [3]. Carbides formed within the DER region have an irregular shape/diffuse boundaries, which are seemingly due to the incomplete *dissolution* of *residual* carbides, which is at odds with the theory of Fu *et al.* and residual carbide growth.

Probing the fundamental mechanisms behind DER formation experimentally have proven difficult and inconclusive. Work needs to be done to understand dislocation-carbon interactions, more specifically, how dislocations can move carbon within the temperature and stress regimes experienced during operation, and what phenomena occur during dislocation-assisted carbon migration. This is vital to understanding martensite decay and DER formation. With further knowledge of the fundamental mechanism behind DER formation, we can surpress dislocation motion in the initial martensitic matrix, mitigating failure by RCF.

To shed light on the fundamental mechanism underpinning DER formation—dislocation-assisted carbon migration—a multi-scale modelling approach can be used. Atomistics can provide information of the 2d Peierls energy landscape which dislocations are subject to in iron; and how this landscape is modified by the binding of carbon to dislocations. This data can be used in a line tension model of a dislocation, to determine the kink-pair nucleation energies of dislocations as a function of carbon content and stress. Finally, one can use a kinetic Monte Carlo model of dislocation glide, by thermally activated kink-pair nucleation, in an environment of carbon. From this last stage of coarse-graining, one can determine in which regimes of temperature, stress and carbon concentration, dislocation-assisted carbon migration

becomes a feasible mechanism behind DER formation; with predictions of dislocation velocity and the motion of carbon as dislocations move. In this report, we will focus on the atomistic portion of this project, focussing on dislocation-carbon interactions at the atomistic scale in bcc iron.

With this work as a foundation, one should be able to compare the affinity of carbon to dislocations/grain boundaries: specifically carbides and grain boundaries, clarifying if carbides grow, as in the theory by Fu, or if they dissolve, as some optical data suggests.

2 Computational Method

We focus here on atomistic simulations, the first stage in the modelling process of dislocation-driven carbon migration.

We use the tight-binding model of Paxton and Elsätter [4], which has been shown to describe the binding energies of carbon complexes in bcc iron, in accordance with high-quality Density Functional Theory (DFT) calculations. Furthemore, this model reproduces the two screw dislocation core structures—the easy and hard $1/2\langle 111$ cores—exhibited in bcc iron, which are crucial to understanding solute-dislocation interactions in bcc iron. Hydrogen and carbon have been shown to reconstruct these cores into the, usually metastable, hard core from the easy core [5, 6]. Cheaper models, which do not incorporate quantum mechanics, such as the EAM, cannot reproduce these behaviours.

This model was used to obtain the 2d Peierls potential of a $1/2\langle 111$ screw dislocation, by simulation of a periodic array of dislocation quadrupoles with the subtraction of interaction energies. Clusters of single dislocations, of both hard and easy cores, were used to determine the binding energy of carbon to the dislocations, and where carbon will be and is preferentially located around each core.

3 Results

3.1 Peierls Potential

To determine the Peierls potential, we followed the procedure detailed in Itakura [7]. Quadrupolar arrays of dislocations were constructed by placing dislocations of antiparallel $1/2\langle 111\rangle$ Burgers vectors in an "S" arrangement [8], see **??**, with initial displacements determined by the anisotropic elasticity solutions. These displacements were modified to be periodic, thereby removing artificial stacking faults which would appear between periodic images after the introduction of the dislocation dipole. This was achieved by the subraction of a linear error term from the superposition of displacement fields arising from the dislocations in the simulation cell and its periodic

images [9]. To accomodate for the internal stress upon introduction of the dislocation dipole into a simulation cell, an elastic strain was applied to the cell, resulting in an additional tilt component added to the cell vectors [8, 9]. Simulation cells were constructed with different initial core positions, which were sampled from the triangular region "EHS" (easy, hard and split) core positions, as detailed in **??**. To fix the dislocation positions during relaxation, the three atoms surrounding the easy core, for each dislocation, were fixed in Z coordinate during relaxation. Relaxations were carried out until forces on each atom were less than $1 \times 10^{-3}\mathrm{eV}^{-1}$.

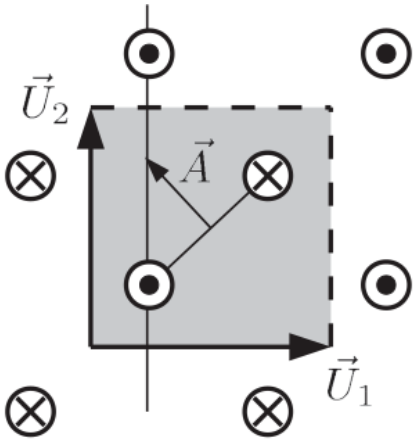

Figure 2: Figure of the quadrupolar arrangement used to determine the Peierls potential. $\vec{U}_1$ and $\vec{U}_2$ are the periodicity vectors in the X-Y plane. $\vec{A}$ is the vector defining the cut plane of the dislocation dipole [8].

The interaction energy between the dislocation dipole and periodic images was defined differently to that of Itakura's. We followed the prescription of Bulatov and Cai [9] to find a regularised interaction energy, which is independent of truncation limit, in contrast to the formulas quoted in Itakura's papers [7]. Details can be found in 7.1.

The Peierls potential here is defined relative to the energy of the easy core configuration. The difference in total energies is taken between a relaxed cell, where the dislocation cores are displaced, from the periodic easy core reference, with a correction term coming from the difference in interaction energies between the displaced state and the easy core, due to the difference in dislocation positions. Δ henceforth refers to quantities relative to the easy core configuration, divided by the total number of dislocations in the reference cell.

$$\Delta E_{\mathrm{P}} = \Delta E^{\mathrm{tbe}} - \Delta E_{\mathrm{INT}}$$

Comparison of 2d Peierls potentials of the $1/2\langle 111\rangle$ screw dislocation between DFT and tight-binding can be found in 1. Data was interpolated

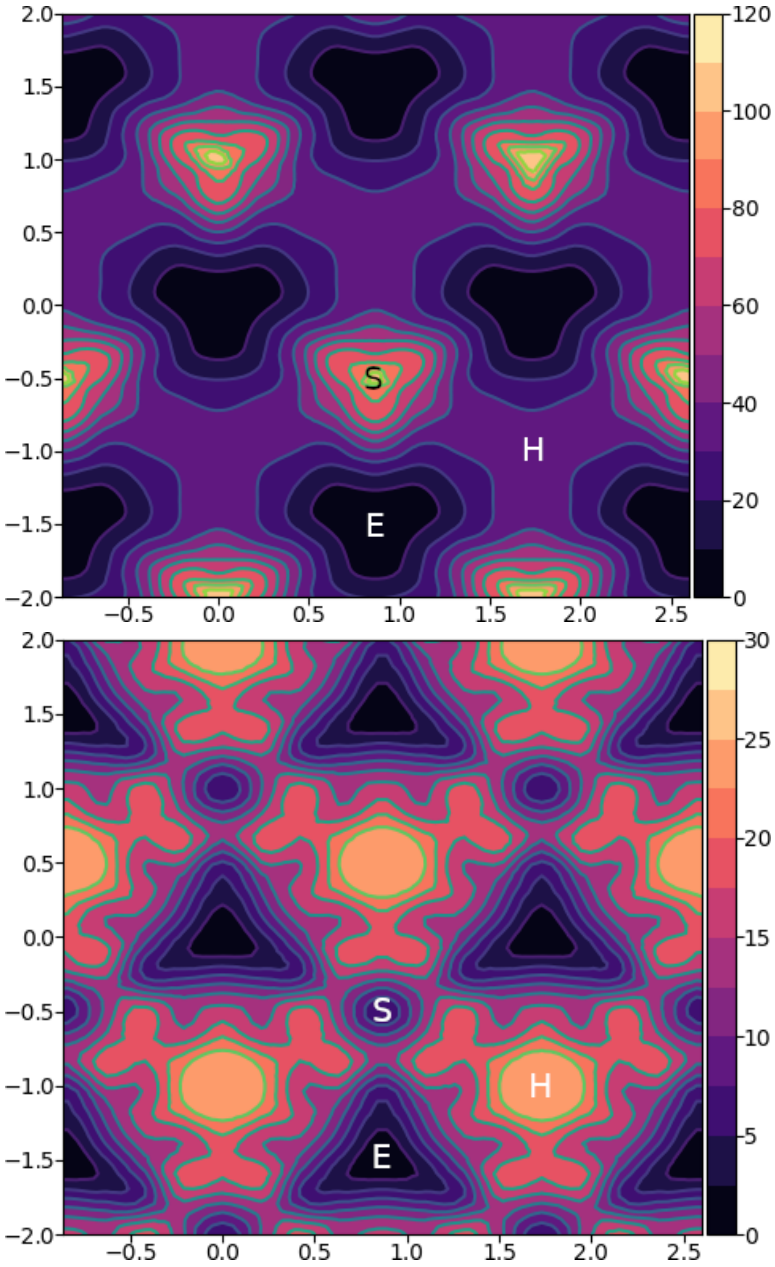

Table 1: Comparison of 2d Peierls potentials of the $1/2\langle 111\rangle$ screw dislocation between DFT cite:Itakura2012 (top) and tight-binding (bottom). Data was interpolated using cubic splines. Energies are in meV, with x and y scales in units of $\sqrt{2}a_{\mathrm{bcc}} = 2\sqrt{2/3}b$. "E", "H" and "S" correspond to easy, hard and split core positions respectively, with the latter also corresponting to atomic positions. The relative energies between the different core positions is smaller in tight-binding compared to DFT. The split core as seen in tight-binding is reminiscent of EAM potentials, where the split core energy is lower than that of the hard core. Some of this discrepancy can be attributed to the difference in interaction energy definitions.

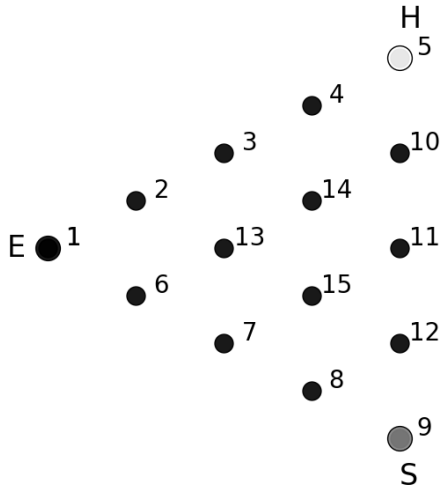

Figure 3: Figure of the sampled positions used to determine the the Peierls potential. "E", "H" and "S" correspond to the easy, hard and split core positions respectively.

using 2d cubic splines. "E", "H" and "S" correspond to easy, hard and split core positions respectively, with the latter also corresponding to atomic positions. The relative energies between the different core positions is smaller in tight-binding compared to DFT; most notably, the energies. This is an artifact in the model, which has been validated in NEB calculations of the $1/2\langle 111\rangle$ screw dislocation Peierls barrier: the tight-binding Peierls barrier half that of DFT [10]. The split core as seen in tight-binding is reminiscent of EAM potentials, where the split core energy is lower than that of the hard core [7]. Some of this discrepancy can be attributed to the to erroneous interaction term included by Itakura, as detailed above—interaction energies can become arbitrarily high, if not made independent of truncation limit—but likely, there are effects in DFT which are not encapsulated fully within tight-binding (or EAM), such as a lack of core electron repulsion or environmental dependence.

Pos	ΔE_{INT}	ΔE_{tbe}	ΔE_{P}	$\Delta E_{\mathrm{P}}^{\mathrm{DFT}}$
1	0	0	0	0
2	-0.7	7.3	7.9	3.2
3	-1.4	16.0	17.4	19.2
4	-2.0	22.2	24.2	31.1
5	-2.5	24.8	27.4	39.3
6	-3.3	3.0	6.3	11.5
7	-6.5	7.1	13.6	39.9
8	-9.6	13.0	22.6	75.2
9	-12.5	5.4	17.9	108.9
10	-4.8	22.1	26.9	34.8
11	-7.2	18.2	25.4	37.9
12	-9.8	14.0	23.8	60.7
13	-3.8	11.5	15.3	17.6
14	-6.9	15.1	22.0	29.9
15	-4.3	18.6	22.9	39.7

3.2 Hard and easy core relaxations

To determine the binding energy of carbon to dislocations, we used the cluster method: simulation cells consist of a cylindrical cluster of atoms, with a single dislocation introduced into the centre using displacements from the anisotropic elasticity solutions. Each of the clusters were centred on the easy or hard core positions. The cluster of atoms was split into two regions: a central region of dynamic atoms with radius R_1, and an annulus of atoms, between R_1 and R_2, which were fixed to the anisotropic elasticity solutions.

Initially, large cells of with $R_1 = 6\sqrt{2}a_{\mathrm{bcc}}$, and $R_2 = 7\sqrt{2}a_{\mathrm{bcc}}$ and depth of single burger's vector, were relaxed for both the easy and hard cores, which consisted of 522 and 540 atoms respectively. The three atoms surrounding the core were constrained, to only relax in $X-Y$ plane, to stop the core from moving upon relaxation. The k-point sampling mesh for each of these cells was 1x1x24, with a charge tolerance for self-consistency of $1e-6$. Atoms were relaxed until the force on each atom was less than 1×10^{-3} eVÅ^{-1}.

From the relaxed cells, a smaller region of 174 atoms, with $R_1 = 3\sqrt{2}a_{\mathrm{bcc}}$, and $R_2 = 4\sqrt{2}a_{\mathrm{bcc}}$, was cut from the dynamic regions. This smaller cell was extended to a thickness of $3b$ in the Z direction. Carbon interstitials were inserted into octahedral sites near the dislocation core, in the middle layer. Exploiting reflection and rotational symmetry, allows us to use only 10 interstitial sites to obtain the binding energies of carbon ~ 2 b from the core.

The three atoms surrounding the core in the first and third layers were again constrained to relax only in the X and Y directions. No such constraints were imposed on the middle layer.

The core energy difference can be estimated by the difference between the

excess energies of the easy and hard cores in the limit that $\ln\frac{R}{R_0}) \to 0$. At the smallest value, one finds that the core energy difference $\Delta E_c^{\text{Easy-Hard}} = 76$ meV/b. This is in agreement with the results of Itakura [7], of 82 meV/b.

As found in DFT simulations by Ventelon [5], when a carbon was placed in the vicinity of a relaxed easy dislocation core—in either of the two nearest, distinguishable, octahedral sites—a spontaneous reconstruction of the dislocation core occurred: from easy to hard. Upon reconstruction, the dislocation core moved to a neighbouring triangle, when looking along the $\langle 111 \rangle$ direction, where the carbon found itself situated in the centre: a prismatic site. This model successfully reproduces this behaviour, confirming that both hard and easy dislocation cores must be studied to fully understand screw dislocation behaviour in bcc iron.

To validate the simulation method, the excess energy, defined as the difference in energy between a cell with a dislocation, and a perfect reference cell, was plotted as as function of $\ln(R/r_c)$, where $R = R_2$ of the cluster and $r_c = b$, is the core radius. In elasticity theory, this should give a linear dependence where the gradient corresponds to combinations of elastic constants. This is well reproduced by our model, except at low $\ln(R/r_c)$ as expected, where the cell size is not large enough to accommodate for sufficient relaxation of the dislocation cores, hence the the core energy increases. Elasticity theory cannot describe the core energy, hence the deviation.

Following the paper by Itakura [6] we calculated the binding energy of carbon each of the screw dislocation cores.

The solution energy is given by

$$E_s = E_{\text{d + C}} - E_{\text{d}} - E_{\text{C ref.}},$$

where $E_{\text{d + C}}$ is the total energy of a relaxed cluster with a carbon interstitial and a dislocation, E_{d} is the total energy of a relaxed cluster with a dislocation and $E_{\text{C oct.}}$ is the total energy of relaxed a cluster with a single carbon in an octahedral site.

The zero-point energy is calculated as in Itakura. After relaxation of the C-dislocation system, a 3x3 Hessian matrix is constructed by taking the numerical derivative of forces observed on the carbon atom after displacement by ± 0.015 in each of the X, Y and Z directions. The three atoms surrounding the core on the first and third layers were again fixed in Z coordinate. The zero-point energy is given by

$$E_z = \frac{1}{2} \sum_{i=1}^{3} \frac{h}{2\pi} \sqrt{k_i / m_{\text{C}}},$$

where k_i are the eigenvalues of the Hessian and m_{C} is the mass of carbon.

The ZPE corrected solution energy is given by

$$E_s^{\text{Z}} = E_s + \Delta E_z,$$

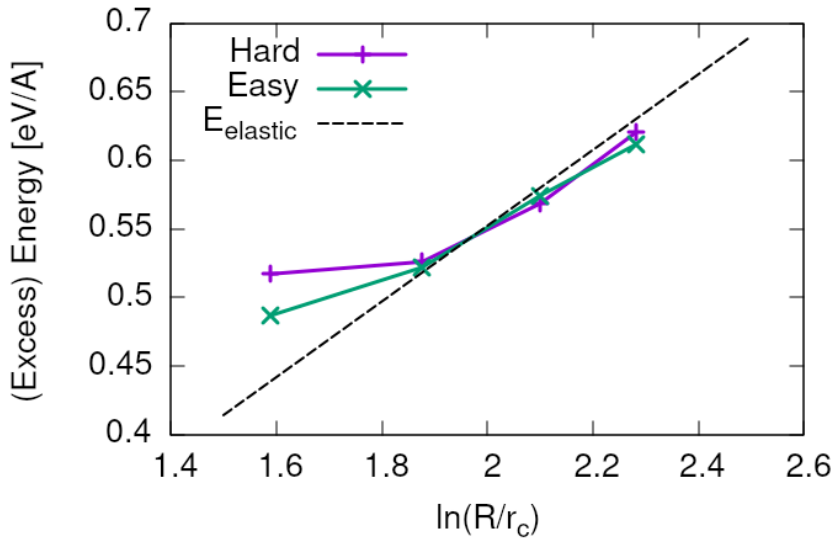

Figure 4: Excess energy of dislocation clusters with differing radii for both the easy and hard core configurations. The prediction from elasticity theory is given by the black, dashed line. Deviation of both cores occur when cell size is small, creating an increase in the core energy, which elasticity theory cannot account for.

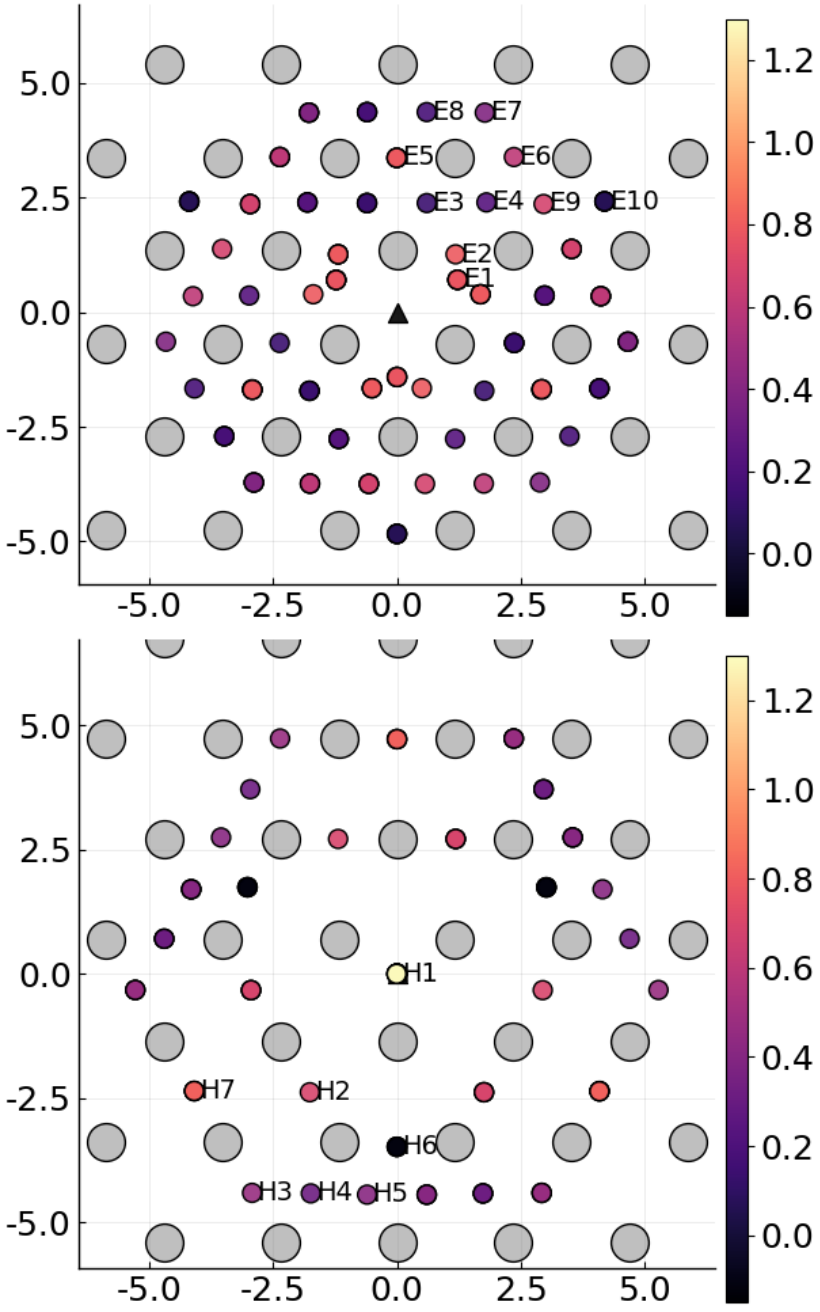

Table 2: Final positions and binding energies (eV) of carbon around the easy core (top) and hard core (bottom). The core was constrained by fixing the top and bottom three atoms surrounding each of the cores. As shown by Ventelon [5], the first and second closest octahedral sites to the hard core have their minimum energy inside the hard core.

Site Type	distance from core [b]	E^z [eV]	ΔE^z [eV]	E_b [eV]	E_b^z [eV]
E1	0.57	0.185	-0.018	0.793	0.775
E2	0.70	0.202	-0.001	0.793	0.793
E3	0.99	0.205	0.002	0.137	0.139
E4	1.21	0.208	0.005	0.229	0.234
E5	1.36	0.210	0.008	0.784	0.791
E6	1.66	0.209	0.007	0.597	0.603
E7	1.89	0.206	0.003	0.385	0.388
E8	1.77	0.203	0.000	0.177	0.178
E9	1.52	0.201	0.000	0.683	0.683
E10	1.95	0.202	0.000	0.067	0.067
H1	0.00	0.196	-0.006	1.298	1.291
H2	1.19	0.210	0.007	0.691	0.698
H3	2.12	0.209	0.007	0.461	0.467
H4	1.91	0.207	0.005	0.311	0.316
H5	1.80	0.208	0.006	0.403	0.409
H6	1.40	0.207	0.005	-0.119	-0.114
H7	1.35	0.206	0.006	0.825	0.819

Table 3: Table of energies leading to the zero-point energy corrected binding energy.

where $\Delta E_z = E_z - E_{z\text{C ref.}}$ and $E_{z\text{C ref.}} = 202.5meV$ is the zero-point energy of carbon situated in an octahedral site in a perfect cluster of the same size. The difference in zero-point energy was found to be negligible in comparison to the binding energies, as one would expect from an atom much larger than hydrogen.

These binding energies agree well with experiment and previous calculations. The maximum binding energy found by the Fe-C EAM potential by Becquart [11], was 0.41eV. Kamber *et al.* found a maximum binding energy of 0.5 eV. Cochardt found a value of 0.71 eV, which is within 0.1eV of the largest binding energy for the easy core.

EAM calculations by Clouet [12] found a binding energy of —- by calculating the elastic dipole tensor within Eshelby theory. Hanlumyuang *et al.* [13] conducted DFT calculations for the interaction energy 12Å from the core, and their calculations agreed with the continuum limit of Eshelby theory with —-.

In work by Ventelon [5], the interaction energy of a carbon in a hard core prism configuration was found to be 0.79eV for a thickness in the Z direction of $3b$ (0.73eV for $6b$)—in the convention that a positive binding energy indicates attraction. This is significantly lower than the 1.29eV interaction energy of tight-binding. This discrepancy can be partially explained due to the short cutoff of the carbon interactions in tight-binding—at $\sim a_{\text{bcc}} = 2.87$.

In addition, these cells are not fully relaxed, as the three atoms around the core are fixed in Z. As the carbon is separated from its periodic image by $3b = 8.61$, there is no contribution from the repulsive C-C interaction from periodic images, which is included within DFT.

In the mean-field model of Ventelon, we have

$$E_{\text{int}}(c_d) = E_{\text{int}}^{(0)} + \frac{\Delta E_{\text{Easy-Hard}}}{c_d} + c_d V_{\text{CC}},$$

where V_{CC} is the C-C interaction energy which can be found by the equation. In tight-binding $V_{\text{CC}} = 0$,

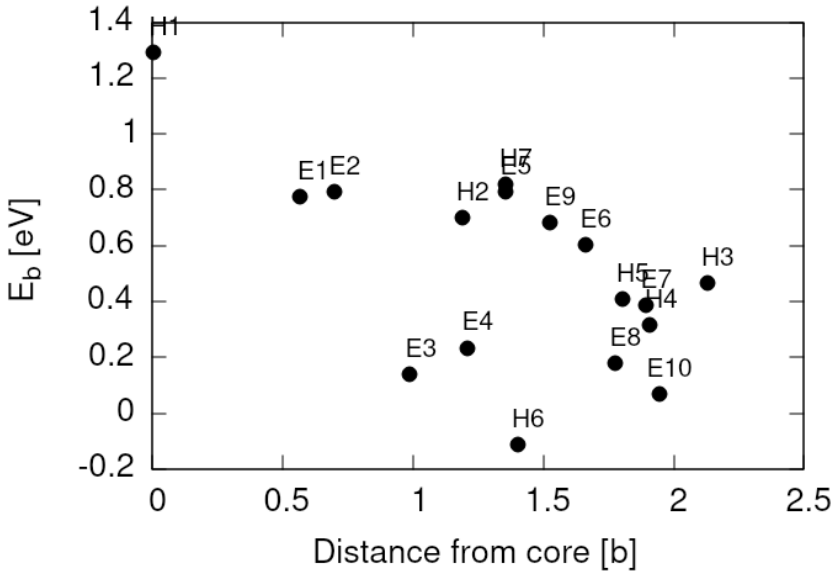

Figure 5: Distance dependence of the binding energies of carbon to the 1/2111 screw dislocation in iron. Positive binding energies denote a favourable binding.

We therefore propose a different mechanism,

3.3 Line Tension

From the atomistic calculations of the Peierls potential and carbon-dislocation binding energies, one can make a line tension model of a dislocation from which we can obtain the kink-pair formation energies as a function of stress and carbon content. This model views the dislocation as an elastic string which moves on the Peierls potential ΔE_{P}.

The dislocation is modelled as a discretised line, with layer labels j. The energy of a dislocation line in the line tension model is given by:

$$E_{\mathrm{LT}} = \frac{K}{2}\sum_{j}(\vec{P}_j - \vec{P}_{j+1})^2 + \sum_{j}\Delta E_{\mathrm{P}}(\vec{P}_j) + (\sigma\cdot\vec{b})\times\vec{l}\cdot\vec{P}_j - \sum_{j,k} E_{\mathrm{C}}(|\vec{P}_j - \vec{P}_k{}^{\mathrm{C}}|),$$

where K is a constant calculated from the model, ΔE_{P} is the Peierls potential, σ is the stress applied, $\vec{b}$ is the burger's vector, with the dislocation line sense given by $\vec{l}$. $\vec{P}_j$ corresponds to the dislocation core position in a given layer, with $E_{\mathrm{C}}(|\vec{P}_j - \vec{P}_k{}^{\mathrm{C}}|)$ being the binding energy of a particular carbon k, at position $\vec{P}_k^{\mathrm{C}}$, to a dislocation positioned at $\vec{P}_j$.

The K coefficient was calculated from atomistic simulations, using the prescription of Itakura [7], calculating a hessian from the displacement of atoms surrounding the dislocation core, giving results of $K = 0.734$ eVÅ^{-2}, compared to DFT $K = 0.816$ eVÅ^{-2}.

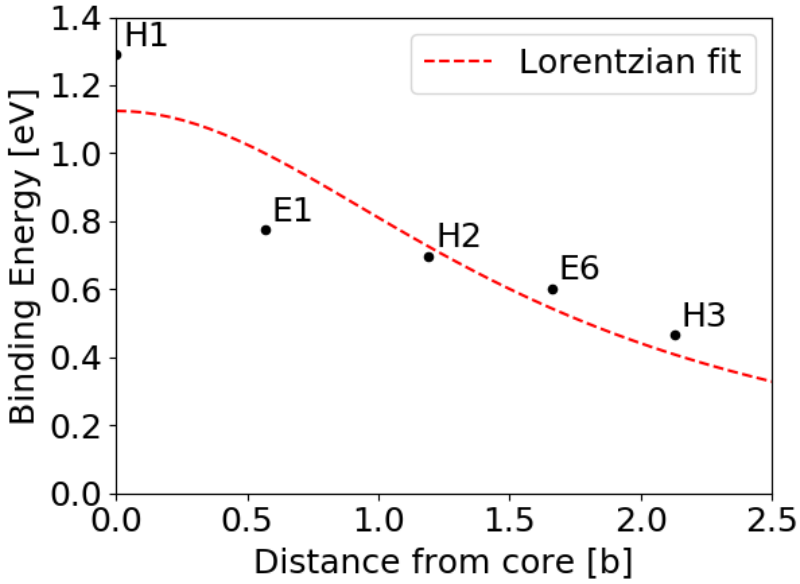

Figure 6: Fit of lorentzian to carbon-dislocation binding energies. The sites chosen to fit to were determined by those sites a prismatic carbon in a hard core configuration would find itself, if the dislocation were to move without it along the $X = \bar{2}111$ direction.

The distance dependence of the dislocation-carbon binding energies, as seen in **??** and **??**, can be fit by a single lorentzian, as was done in Itakura—but with the ommision of many binding energies, as is done in . To take more of the atomistic data into account in the line tension model, we propose another method to be used in further work.

Upon movement of a screw dislocation saturated with carbon, for example, the expected hard core ground state configuration (with Hx sites filled) to an adjacent easy core position, it is expected that carbon will not diffuse away in the time it takes for the dislocation to move position, due to the large dislocation velocity compared to the speed of diffusivity in carbon. So sites occupied by carbon will remain in the same position relative to the lattice as the dislocation changes to the easy core. This results in a new dislocation-carbon configuration. If the carbon is near one of the positions of the Ex sites, it will decay to that position, resulting in a new carbon-dislocation binding energy, which is now of easy core type. One can linearly interpolate between these binding energies, depending dislocation core position.

- Show line tension work maybe?
- Inconclusive right now as more work needs to be done.
- Explain the interpolation between the easy and hard cores, for where it is possible, otherwise, fit a lorentzian!

Validation tests of the solute-dislocation interaction within the line tension model will be carried out on the Itakura data set for the binding of hydrogen to screw dislocations in bcc iron. This will be used to verify the kink-pair formation enthalpies stated in their paper (using the lorentzian form of the dislocation-solute interaction energy). This data set will also be used to verify the new interpolated solute-dislocation interaction energy, between the hard and easy core configurations.

The julia implementation of the NEB/string algorithms was used [14]. One finds that the line shapes are similar to that of Itakura.

4 Discussion

- How do the results of this work feed into C migration with dislocations?
- How valid is the theory we have vs Fu *et al.*
- Novel work to find out dislocation environment around both dislocation cores.

  As in [15], carbon interactions are found to be vital in understanding how screw dislocations move in steels. Due to the spontaneous reconstruction of the easy core upon introduction of carbon, and the large binding energy of the H1 site, one would expect a hard core with carbon in a prismatic site as the ground state configuration for pinned dislocations. With stress, the dislocation will be forced to move (say, along the $X = \bar{2}11$ direction), which results in the hard core reconstructing

to an easy core. Due to the much higher velocity of dislocations, relative to the diffusivity of carbon, one expects carbon in the prismatic site will not move, becoming an E1 site. This hinders motion due to the drag force acting on the dislocation, due to the binding of the carbon in the E1 site. Further motion results in the dislocation core structure becoming hard again, with the original carbon now being a H2 site, with a different drag force. Additional movement results in the carbon being situated in E6 and then H3 sites, after easy and hard core reconstructions.

This forms the basis of the line tension model of the dislocation. We have a more sophisticated method of being able to incorporate the binding energy of carbon to dislocations than Itakura.

- Peierls potential agrees, although it is low compared to DFT
- Line tension model has been set up, although results have not been achieved yet.
- kMC depends on the results of the line tension model.

The first stage in this work is

5 Future work

- Validation of line-tension model by reproduction of the dislocation line shape from Itakura 2012 [7].
- Compare tbe dislocation line shape with Itakura, and find the migration path of the dislocation from tbe data.
- [Optional] Create Ising model for easy and hard core an compare the binding energies like [15].
- [Optional] Find the elastic dipole tensor to check the binding energy of C within anisotropic elasticity.
- Choose the sites for which one can fit a function (lorentzian) for the interaction energy between C and Fe.
- Find the kink-pair formation enthalpy, with and without carbon, to feed into the kMC code.

6 Conclusion

- Outline of the literature review

1. Origin of DER formation through high-cycle fatigue
2. What is the DER region and what phases is it composed of?
3. What are the current mechanisms which explain this?
   (a) Why are they insufficient?
4. Ouline of the work considering Fe-C dislocation modelling

7 Appendix

7.1 Regularisation of interaction energy in quadrupolar array

In isotropic elasticity, the elastic energy of a single dislocation dipole in an infinite lattice is given by

$$E_{\text{el}}^{\infty} = \frac{\mu b^2}{4\pi} ln(\frac{r}{r_c})$$

The contribution from periodic images to the correction is

$$E_{\text{img}} = E_{\text{el}}(\mathbf{a}, \mathbf{c}_i, r_c) - E_{\text{el}}^{\infty}(\mathbf{a}, r_c),$$

"Ghost" dipoles are introduced to account for the conditional convergence of the sum at $\pm\alpha\mathbf{b}$ and $\pm\beta\mathbf{b}$, where $\alpha = \beta = 0.5$. We define $E_{\text{dg}}(\mathbf{R})$ as the interaction energy of a ghost dislocation and a dipole at $\mathbf{R}$ anisotropic elasticity equations as shown in [16].

Defining,

$$E_{\text{dd}}(\mathbf{R}) = \frac{\mu b^2}{2\pi} \ln \frac{|\mathbf{R}|^2}{|\mathbf{R}+\mathbf{a}| \cdot |\mathbf{R}-\mathbf{a}|},$$

we obtain,

$$E_{\text{img}} = \frac{1}{2} \sum_{\mathbf{R}} [E_{\text{dd}}(\mathbf{R}) - E_{\text{dg}}(\mathbf{R})] - \frac{1}{2} E_{\text{dg}}(\mathbf{R} = 0),$$

which can be subtracted from the total energy as given from atomistic calculations, for a regularised interaction energy.

8 Bibliography

References

[1] H. Fu, E.I. Galindo-Nava, and P.E.J. Rivera-Díaz del Castillo. Modelling and characterisation of stress-induced carbide precipitation in bearing steels under rolling contact fatigue. *Acta Materialia*, 128:176–187, April 2017.

[2] Hanwei Fu, Wenwen Song, Enrique I. Galindo-Nava, and Pedro E.J. Rivera-Díaz del Castillo. Strain-induced martensite decay in bearing steels under rolling contact fatigue: Modelling and atomic-scale characterisation. *Acta Materialia*, 139(nil):163–173, 2017.

[3] H. K. D. H. Bhadeshia. Solution to the bagaryatskii and isaichev ferrite–cementite orientation relationship problem. *Materials Science and Technology*, 34(14):1666–1668, May 2018.

[4] A. T. Paxton and C. Elsässer. Analysis of a carbon dimer bound to a vacancy in iron using density functional theory and a tight binding model. *Physical Review B*, 87(22), June 2013.

[5] Lisa Ventelon, B. Lüthi, E. Clouet, L. Proville, B. Legrand, D. Rodney, and F. Willaime. Dislocation core reconstruction induced by carbon segregation in bcc iron. *Physical Review B*, 91(22), June 2015.

[6] M. Itakura, H. Kaburaki, M. Yamaguchi, and T. Okita. The effect of hydrogen atoms on the screw dislocation mobility in bcc iron: a first-principles study. *Acta Materialia*, 61(18):6857–6867, 2013.

[7] M. Itakura, H. Kaburaki, and M. Yamaguchi. First-principles study on the mobility of screw dislocations in bcc iron. *Acta Materialia*, 60(9):3698–3710, May 2012.

[8] Emmanuel Clouet. Screw dislocation in zirconium: An ab initio study. *Physical Review B - Condensed Matter and Materials Physics*, 86(14):1–11, 2012.

[9] Vasily Bulatov. *Computer Simulations of Dislocations (Oxford Series on Materials Modelling)*. Oxford University Press, dec 2006.

[10] E. Simpson. *A Tight Binding Study of Dislocations in Iron and Their Interactions with Hydrogen*. PhD thesis, King's College London, 2019.

[11] C.S. Becquart, J.M. Raulot, G. Bencteux, C. Domain, M. Perez, S. Garruchet, and H. Nguyen. Atomistic modeling of an fe system with a small concentration of c. *Computational Materials Science*, 40(1):119–129, July 2007.

[12] Emmanuel Clouet, Sébastien Garruchet, Hoang Nguyen, Michel Perez, and Charlotte S. Becquart. Dislocation interaction with c in -fe: A comparison between atomic simulations and elasticity theory. *Acta Materialia*, 56(14):3450–3460, August 2008.

[13] Y. Hanlumyuang, P.A. Gordon, T. Neeraj, and D.C. Chrzan. Interactions between carbon solutes and dislocations in bcc iron. *Acta Materialia*, 58(16):5481–5490, September 2010.

[14] Stela Makri, Christoph Ortner, and James R. Kermode. A preconditioning scheme for minimum energy path finding methods. *The Journal of Chemical Physics*, 150(9):094109, March 2019.

[15] B Lüthi, F Berthier, L Ventelon, B Legrand, D Rodney, and F Willaime. Ab initio thermodynamics of carbon segregation on dislocation cores in bcc iron. *Modelling and Simulation in Materials Science and Engineering*, 27(7):074002, July 2019.

[16] Wei Cai, Vasily V. Bulatob, Jinpeng Chang, Ju Li, and Sidney Yip. Periodic image effects in dislocation modelling. *Philosophical Magazine*, 83(5):539–567, January 2003.